Published in IET Nanobiotechnology
Received on 23rd February 2013
Revised on 25th June 2013
Accepted on 25th June 2013
doi: 10.1049/iet-nbt.2013.0012

ISSN 1751-8741

Single walled boron nitride nanotube-based biosensor: an atomistic finite element modelling approach

Mitesh B. Panchal, Sanjay H. Upadhyay

Vibration and Noise Control Laboratory, Mechanical and Industrial Engineering Department, Indian Institute of Technology Roorkee, Roorkee 247667, Uttarakhand, India
E-mail: miteshbpanchal77@gmail.com

Abstract: The unprecedented dynamic characteristics of nanoelectromechanical systems make them suitable for nanoscale mass sensing applications. Owing to superior biocompatibility, boron nitride nanotubes (BNNTs) are being increasingly used for such applications. In this study, the feasibility of single walled BNNT (SWBNNT)-based bio-sensor has been explored. Molecular structural mechanics-based finite element (FE) modelling approach has been used to analyse the dynamic behaviour of SWBNNT-based biosensors. The application of an SWBNNT-based mass sensing for zeptogram level of mass has been reported. Also, the effect of size of the nanotube in terms of length as well as different chiral atomic structures of SWBNNT has been analysed for their sensitivity analysis. The vibrational behaviour of SWBNNT has been analysed for higher-order modes of vibrations to identify the intermediate landing position of biological object of zeptogram scale. The present molecular structural mechanics-based FE modelling approach is found to be very effectual to incorporate different chiralities of the atomic structures. Also, different boundary conditions can be effectively simulated using the present approach to analyse the dynamic behaviour of the SWBNNT-based mass sensor. The presented study has explored the potential of SWBNNT, as a nanobiosensor having the capability of zeptogram level mass sensing.

1 Introduction

Recently, nanotubes, nanowires, fullerenes and nanoparticles have come out as a new class of materials for biosensing and medical diagnostics applications [1–4]. Detailed understanding of the nature, physical and chemical mechanisms, structure and spatial distribution of conjugating molecules and nanomaterials is critically important to capitalise the novel properties of nanobioconjugates [5]. In the case of nucleobases of DNA and RNA, it has been shown that the *N*-site is the preferred site for forming a stable bioconjugate complex with metallic [6] and semiconducting quantum dots [7]. The mass detection of biomolecules has become a growing field in biological and biomedical applications. It is recognised as one of the key technologies for predictive and preventive medicine [8]. The common strategy for prediction of disease is based on sensing the corresponding biomolecules [8]. It is reasonable to believe that biosensors with real-time sensing capability and ease of use can change the future of disease detection and health monitoring.

Boron nitride nanotubes (BNNTs), possess a similar atomic structure as that of carbon nanotubes (CNTs) in which alternating B and N atoms entirely substituted for C atoms. Having distinct properties of their own, BNNTs appear to be potential candidates for biomedical applications because of their stability in dispersion in solution. Unlike CNTs, BNNTs are semiconducting regardless of their diameter and chirality [9]. BNNTs are also found to be non-toxic to health as well as environment because of their chemical and structural stability, and therefore they are more suitable for medical applications such as biosensors.

Several literatures can be found addressing the application of nanotubes in biotechnology, in comparison to CNTs, the use of BNNTs have not been enlightened largely [10]. Ciofani *et al.* [11] experimentally studied the suitability of BNNTs in the field of nanomedicine and reported that BNNTs are more suitable for development of sensors for detection of biological entities, because of their chemical inertness. The operational principle of such nanosensor devices is to detect deposited biomass in terms of shift in frequency or change in conductance [12–15]. Braun *et al.* [16] had theoretically predicted and experimentally validated the mass sensing capabilities of micromechanical cantilevered mass sensors for biomolecular detection in physiological environment. Joshi *et al.* [17] had explored the suitability of CNT-based biosensor for zeptogram-level mass detection. Kuang *et al.* [18] had theoretically predicted and experimentally validated single walled CNT field effect transistors as ideal candidates for creation of chemosensors. Farmanzadeh and Ghazanfary [19] had investigated the interaction between glycine molecule with the zigzag form (6, 0) of single walled BNNTs (SWBNNTs) in the presence and absence of electric field using density function theory and reported useful design

criteria for development of nanosensors, that absorption of glycine on BNNT could be controlled by the intensity of the electric field. Chowdhury and Adhikari [20] had theoretically derived sensor equations using continuum-beam theory for the cantilevered and bridged configurations of BNNTs and validated using molecular mechanics simulations and concluded that BNNTs can be used as biosensor with sensitivity reaching in the order of 0.1 zg/GHz. The present available literatures have explored the feasibility of nanotube based bio-sensing considering change in resonant frequency because of the nanoscale mass at the free end of the nanotube for the cantilevered configuration and at the middle of the length for bridged configuration of SWBNNT [17, 20]. For the resonant frequency shift-based mass sensing the landing position of the added mass along the length of the nanotube is equally important. In higher-order modes of vibrations, the occurrence of maximum displacement at two or more positions along the length of nanotubes are possible and different intermediate landing position of added mass along the length of nanotube can result in different resonant behaviour of the nanotube-based mass sensor [21, 22].

In the present work, the feasibility of SWBNNT-based biosensors has been explored considering finite element (FE) modelling of SWBNNTs. The molecular structural mechanics-based FE model of SWBNNT is developed considering beam elements and point masses. The mechanical properties of beam elements, which represent BN bonds are used based on the mechanical behaviour of BN bond under bond stretching, in-plane rotation and torsional deformations (bond dihedral rotation and hinging deformation) [22, 23]. The concentrated masses with boron nuclei masse ($m_b = 1.7950 \times 10^{-26}$ kg) and nitrogen nuclei masse ($m_n = 2.3258 \times 10^{-26}$ kg) are considered as point masses for the present FE model of SWBNNT. The feasibility of the SWBNNT-based biosensor has been explored considering the two types of biological objects, alanine with amino terminal residue having mass of 0.121307 zg (a type of α-amino acid with simple structure) and deoxyadenosine with free residue having mass of 0.416965 zg (a nucleoside component of DNA composed of adenosine and deoxyribose). The presented FE model-based simulation approach is validated with the molecular mechanics based computations results obtained by Chowdhury and Adhikari [20]. Using the present FE model, different chiral atomic structures of SWBNNT can be effectively simulated to analyse their dynamic behaviour. The effect of chirality on the resonant behaviour of SWBNNT-based biosensors has been analysed for SWBNNTs of diameter 0.6924 nm and having different chiral structures such as (6, 4), (7, 3), (7, 2) and (8, 1) having chiral angle of 23.41°, 17.00°, 12.22° and 5.81°, respectively. Also, considering the present FE modelling approach as different boundary conditions can be effectively simulated, the intermediate landing positions of the added mass along the length of the nanotube have been analysed considering higher-order modes of vibrations. The single molecule of alanine with amino terminal residue is considered at different intermediate positions '*a*' from the fixed end of the armchair (4, 4) form of SWBNNT having diameter 0.551 nm and length $L = 9.99$ nm. The obtained results indicate the feasibility of SWBNNT-based biosensing having detection capability of a biological object of the zeptogram mass scale as well as identification of its intermediate landing position along the length of the nanotube.

2 Atomic structure of SWBNNT

Fig. 1 shows the lattice indices of translation (n, m) along the base vectors, $\boldsymbol{a}_1$ and $\boldsymbol{a}_2$. The n and m are the indices of translation which decide the structure around the circumference. The value of index translation $m = 0$ and $m = n$ results in zigzag and armchair forms of SWBNNTs, respectively. SWBNNTs are formed by rolling an h-BN sheet about the $\boldsymbol{R}$ vector. A vector perpendicular to the $\boldsymbol{R}$ is the chiral vector denoted by $\boldsymbol{C}_h$. The chiral vector and corresponding chiral angle define the type of SWBNNTs, that is, zigzag, armchair and chiral. With respect to two base vectors $\boldsymbol{a}_1$ and $\boldsymbol{a}_2$ the chiral vector, $\boldsymbol{C}_h$ and chiral angle, θ can be expressed as under

$$\boldsymbol{C}_h = n\boldsymbol{a}_1 + m\boldsymbol{a}_2 \tag{1}$$

and chiral angle θ

$$\cos\theta = (n + (m/2))/\sqrt{n^2 + nm + m^2} \tag{2}$$

3 FE modelling of SWBNNT

Moon and Hwang [24] investigated the optimised structure of BN nanotubes based on universal force field (UFF) and reported BN bond length of 0.1432, 0.144, 0.1543 and 0.1559 nm for the structural data of borazine, h-BN, N-dimethylaminodiborane and c-BN, respectively. Boldrin *et al.* [23] proposed energy equivalence principles-based analytical formulation for the in-plane mechanical properties of h-BN nanosheets and reported equilibrium length of BN bond 0.145 and 0.153 nm using DREIDING and UFF force models, respectively. In the present work, the effect of chirality on the resonant behaviour of SWBNNT-based biosensor is analysed for the fixed size (diameter and length) of nanotube. The constant value of

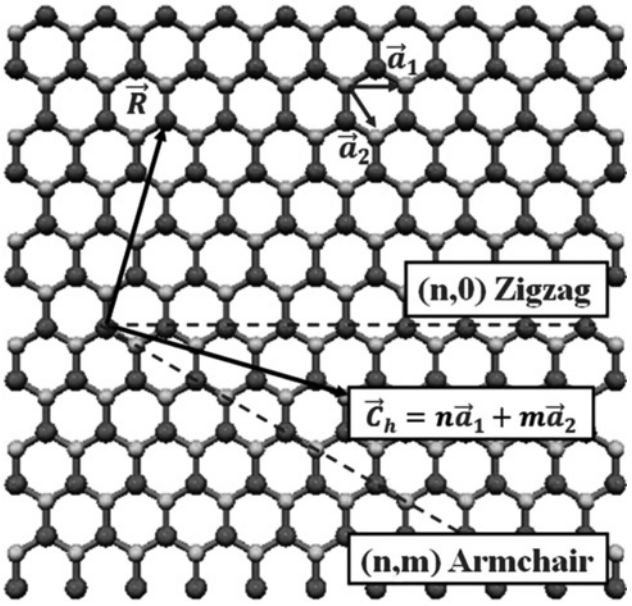

Fig. 1 *Hexagonal lattice of h-BN nanosheet and base vector for rolling of different forms of nanotubes*

doi: 10.1049/iet-nbt.2013.0012

BN bond length for different chiral atomic structures of nanotube results in nanotubes of different diameters and consequently this variation in size alters the resonant behaviour of the nanotube, which is due to change in chirality as well as change in size of the nanotube. This may result in wrong interpretation of the effect of chirality on resonant behaviour of the nanotube. For this reason, the constant size of nanotubes are considered to analyse the chirality effect on resonant behaviour. Different chiralities using the present atomistic FE model are simulated considering different possible values of BN bond length. The different possible values of BN bond length are considered within the range of 0.1430 nm (closely packed atomic structure) to 0.1559 nm. Table 1 shows, the different possible values of BN bond length and values of chiral angle θ, for SWBNNTs of diameter 0.6924 nm.

The present FE model has been developed using three-dimensional elastic beam and point masses. The elastic properties of beam elements, which represent BN bonds are considered from the reference results [22, 23]; Young's modulus 0.263 TPa and Poisson's ratio 0.211. The concentrated masses with boron nuclei masses and nitrogen nuclei masses are positioned at the ends of the beam elements representing joints of B–N bonds. In comparison with the mass of nuclei, mass of electrons are not significant, and it is assumed to be negligible. The commercial FEM-based package, is used to model the present FE model of the SWBNNT. Fig. 2 shows the atomic structures as well as the FE models of different chiral atomic structures of SWBNNTs of diameter 0.6924 nm as mentioned in Table 1.

Table 1 Different values of chiral angle θ and BN bond length for different chiral atomic structures of SWBNNT of diameter 0.6924 nm

Chiral SWBNNT type	Chiral angle, θ	BN bond length, nm
(6, 4)	23.41	0.1441
(7, 3)	17.00	0.1430
(7, 2)	12.22	0.1534
(8, 1)	5.81	0.1467

4 Mass-resonant frequency shift relationship for SWBNNT-based mass sensing

The rationale of mass sensing using resonant-based sensor is on the conception that the resonant frequency is sensitive to sensor mass, which includes the self-mass of the sensor and the mass attached on it. The change of the mass attached on the sensor can cause a shift in the resonant frequency. The key issue of mass sensing is in quantifying the change in the resonant frequency because of attached mass. Based on this rationale, the development of computational tools adequate to simulate the vibrational behaviour of BNNT-based mass sensor is important. Application of the beam bending theory can be performed to model the bending vibration of the cantilevered SWBNNT-based sensor systems specially for the BNNT of larger length; as Chopra and Zettl [25] have experimentally observed the bending vibration of cantilevered BNNT using transmission electron microscopy. Also, Suryavanshi *et al.* [26] had reported the possible higher-order modes of vibrations for cantilevered BNNT using scanning electron microscope images.

For an SWBNNT of length L, with attached mass at the free end of the cantilevered configuration, the fundamental frequency based on Euler-Bernoulli theory can be given as [27]

$$f = \frac{1}{2\pi}\sqrt{\frac{k_{\text{eq}}}{m_{\text{eq}}}} \tag{3}$$

where k_{eq} and m_{eq} are the equivalent stiffness and mass of the cantilevered configuration of SWBNNT, respectively.

The equivalent stiffness (k_{eq}) and equivalent mass (m_{eq}) for the cantilevered configuration of nanotube can be obtained as [13, 20, 22]

$$k_{\text{eq}} = \frac{3EI}{L^3} \tag{4}$$

and

$$m_{\text{eq}} = \frac{33}{140}\rho AL + M \tag{5}$$

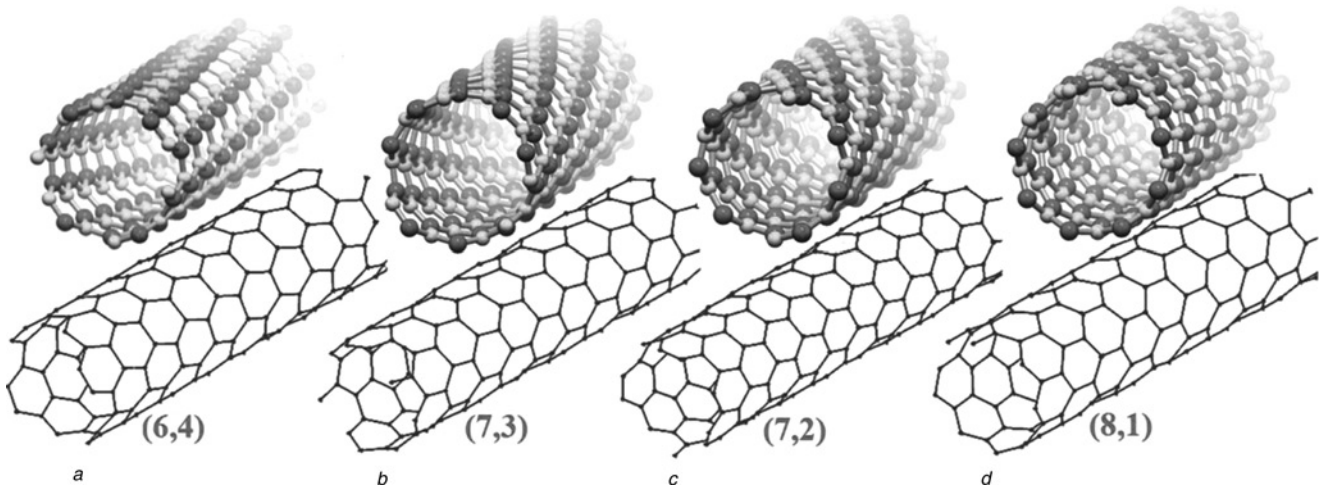

Fig. 2 *Atomic structures and corresponding FE model of different chiral structures*
a (6, 4)
b (7, 3)
c (7, 2)
d (8, 1) of SWBNNTs of diameter 0.6924 nm

Substituting (4) and (5) in (3), the resonant frequency can be obtained as

$$f = \frac{1}{2\pi L^2}\frac{\alpha^2_{\text{cantilevered}}\beta}{\sqrt{1+\Delta M \mu_{\text{cantilevered}}}} \tag{6}$$

where

$$\alpha^2_{\text{cantilevered}} = \sqrt{\frac{140}{11}}, \quad \beta = \sqrt{\frac{EI}{\rho A}}, \quad \Delta M = \frac{M}{\rho A L}$$
$$\text{and } \mu_{\text{cantilevered}} = \frac{140}{33} \tag{7}$$

Resonant frequency with no attached mass for cantilevered configuration of sensor is expressed by considering $\Delta M = 0$ in (6)

$$f_0 = \frac{1}{2\pi L}\alpha^2\beta \tag{8}$$

and resonant frequency shift Δf because of attached mass M can be defined as

$$\Delta f = f_0 - f = f_0 - \frac{f_0}{\sqrt{1+\Delta M \mu}} \tag{9}$$

rearrangement gives expression

$$\Delta M = \frac{1}{\mu\left(1-\left(\Delta f/f_0\right)\right)^2} - \frac{1}{\mu} \tag{10}$$

Using (7), (10) can be used to obtain the relationship, which relates the attached mass and resonant frequency shift as

$$\Delta M = \frac{\rho A L}{\mu}\frac{\left(\alpha^2\left(\beta/L^2\right)\right)^2}{\left(\alpha^2\left(\beta/L^2\right) - 2\pi\Delta f\right)^2} - \frac{\rho A L}{\mu} \tag{11}$$

This is a general equation to relate the attached mass and resonant frequency shift.

5 Results and discussion

5.1 Validation of present FE modelling approach

As shown in Fig. 3, two biological objects having zeptogram scale mass have been used to simulate the resonant behaviour of SWBNNT-based biosensors. Fig. 3*a* is alanine with amino terminal residue; alanine is an α-amino acid with chemical configuration of $CH_3CH(NH_2)COOH$. It is one of the proteinogenic acids. The α-carbon atom of alanine is bound with a methyl group ($–CH_3$), making it one of the simplest α-amino acids with respect to molecular structure and also resulting in alanines being classified as an aliphatic amino acid. The methyl group of alanine is non-reactive and never directly involved in protein function. Alanine can be manufactured in the body from branched chain amino acids such as valine, leucine and isoleusine and it plays a key role in glucose–alanine cycle between tissues and liver. Fig. 3*b* is deoxyadenosine with free residue; deoxyadenosine refers to a deoxyribonucleoside (a component of DNA, composed of adenosine and deoxyribose) with the chemical composition as $C_{10}H_{13}N_5O_3$. It is derived from the nucleoside adenosine, which differs by the replacement of a hydroxyl group (–OH) by hydrogen (–H) in the ribose part of the molecule.

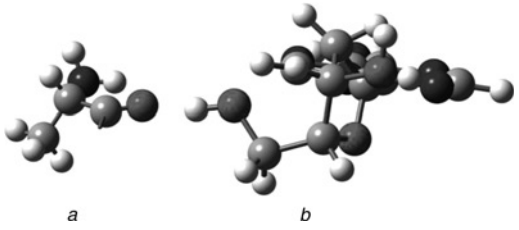

Fig. 3 *Considered biological objects*
a Alanine with amino terminal residue
b Deoxyadenosine with free residue [20]

Fig. 4 shows the FE models of considered zigzag (5, 0) and armchair (4, 4) forms of SWBNNT of cantilevered configurations. The present FE modelling-based simulation approach is validated by comparing the obtained results using the present approach with the molecular mechanics-based computational results obtained by Chowdhury and Adhikari [20]. The cantilevered configuration of zigzag (5, 0) BNNT having diameter 0.389 nm and length 6.922 nm is used for adding upto six molecules of alanine with amino terminal residue at the free end of the nanotube. Cantilevered configuration of armchair (4, 4) BNNT having diameter 0.551 nm and length 9.99 nm is used for adding upto six molecules of deoxyadenosine with free residue. The variation in frequency shift against added mass as the molecular mass of both types of considered biological objects upto six molecules are analysed (Fig. 5). The obtained results are in close proximity to those obtained by Chowdhury and Adhikari [20] for both types of considered biological objects. The percentage error in the results obtained using the present FE model-based simulation approach with respect to the published data are summarised in Tables 2 and 3 for the zigzag as well as armchair cantilevered configurations of SWBNNT-based biosensors. From Tables 1 and 2, it is clear that as the added mass in terms of number of molecules increases for both the considered biological objects, the percentage error between obtained results and reference results decreases.

5.2 Resonant behaviour of SWBNNT-based biosensors

5.2.1 Effect of chiral atomic structures: The effect of different chiral atomic structures on the resonant behaviour of SWBNNT-based biosensor is analysed considering the

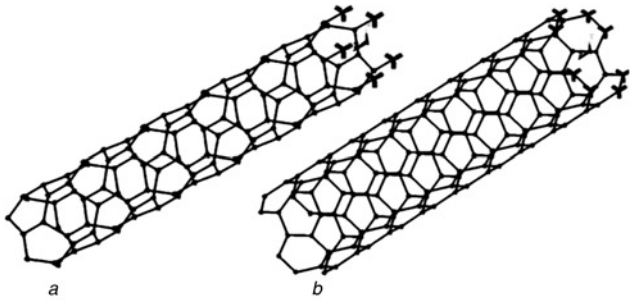

Fig. 4 *FE models of cantilevered configurations of SWBNNTs*
a Zigzag form (5, 0)
b Armchair form (4, 4)

doi: 10.1049/iet-nbt.2013.0012

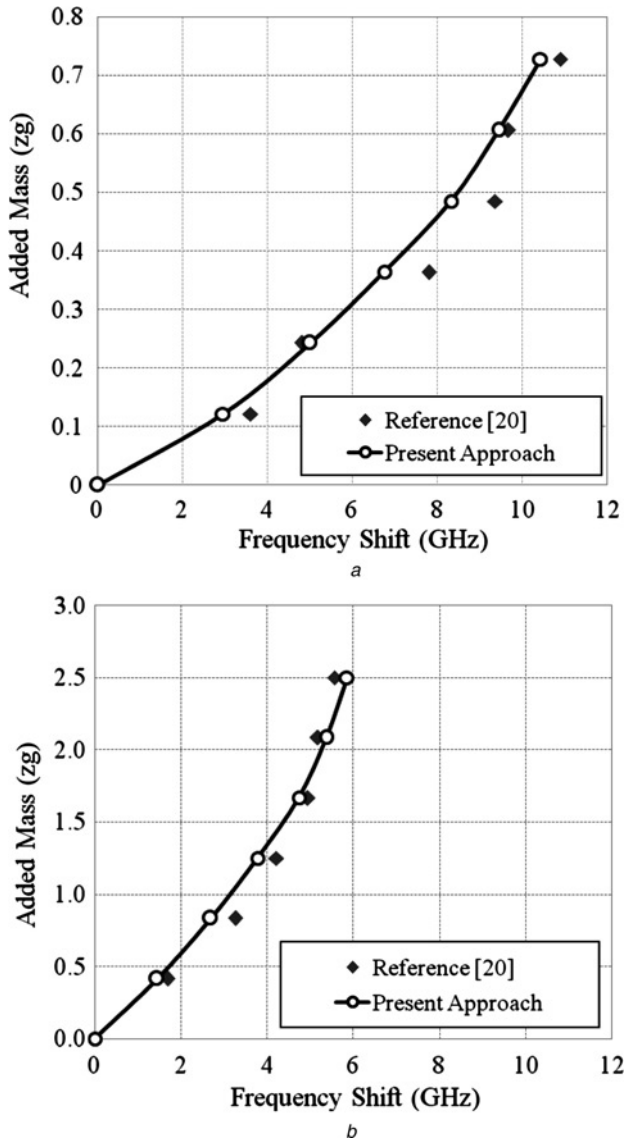

Fig. 5 *Variation in frequency shift against added molecules of considered biological objects (upto six molecules) for a cantilevered configuration of SWBNNT*

a Alanine with amino terminal residue on zigzag (5, 0) BNNT of diameter 0.389 nm and length 6.922 nm
b Deoxyadenosine with free residue on armchair (4, 4) BNNT of diameter 0.551 nm and length 9.99 nm

nanotubes of diameter 0.6924 nm having aspect ratios 10 and 15. Fig. 6 shows the variation in fundamental frequency of the nanotubes of different considered chiral atomic structures of

Table 2 Percentage error in the resonant frequency shift using cantilevered zigzag (5, 0) SWBNNT-based biosensor

Alanine with amino terminal residue, (5, 0) BNNT of diameter = 0.389 nm and length 6.922 nm			
Attached mass, zg	Frequency shift, GHz present FE model approach	Frequency shift, GHz Chowdhury and Adhikari [20]	%Error
0.121307	3.5975	2.9520	21.8665
0.242614	4.7967	4.9980	4.0276
0.363921	7.7946	6.7470	15.5269
0.485228	9.3595	8.3204	12.4886
0.606535	9.6653	9.4424	2.3606
0.727842	10.8885	10.4335	4.3610

Table 3 Percentage error in the resonant frequency shift using cantilevered armchair (4, 4) SWBNNT-based biosensor

Deoxyadenosine with free residue, (4, 4) BNNT of diameter = 0.551 nm and length 9.99 nm			
Attached mass, zg	Frequency shift, GHz present FE model approach	Frequency shift, GHz Chowdhury and Adhikari [20]	%Error
0.416965	1.4420	1.6908	14.7149
0.83393	2.6880	3.2617	17.5890
1.250895	3.7780	4.2091	10.2421
1.66786	4.7400	4.9406	4.0602
2.084825	5.3722	5.1744	3.8219
2.50179	5.8549	5.5611	5.2828

SWBNNT of diameter 0.6924 nm for the aspect ratios 10 and 15. The results indicate that as the chiral angle decreases, fundamental frequency of the nanotube decreases. The variation in fundamental frequency of nanotube can be attributed to change in the orientation of the beam elements of SWBNNT with respect to change in the chiral angle.

As mentioned in Table 1, different chiral structures of SWBNNT; (6, 4) (7, 3) (7, 2) and (8, 1) are considered to analyse the effect of chirality on the resonant behaviour of SWBNNT-based biosensors. The molecular mass of considered biological objects is added upto ten molecules at the free end of the cantilevered configuration of the nanotube. The resonant behaviour in terms of variation in frequency shift against added mass is analysed (see Fig. 7). The obtained results indicate that as the magnitude of added mass increases the frequency shift increases for all the different considered chiral atomic structures of the nanotubes. For nanotubes of aspect ratios 10 and 15, variation in frequency shift because of added mass follows a similar pattern for both the considered biological objects, but the obtained frequency shift for the nanotube of aspect ratio 10 is higher than that for the nanotube of aspect ratio 15. This difference in resonant frequency shift is because of

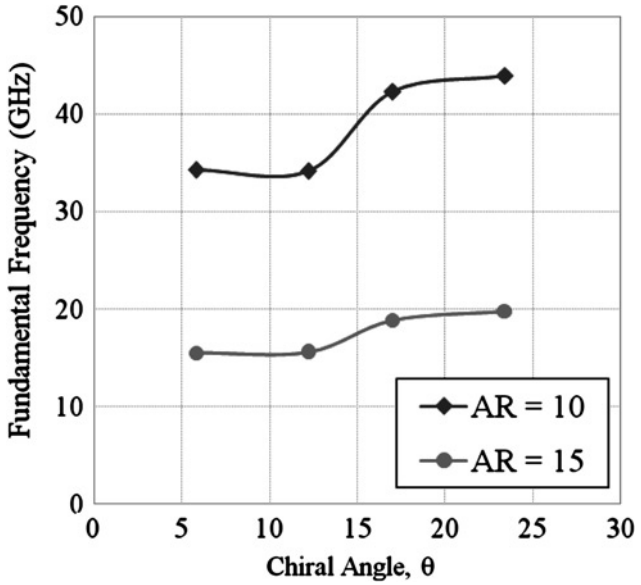

Fig. 6 *Fundamental frequency of SWBNNT of different considered chiral atomic structures of SWBNNT of diameter 0.6924 nm (6, 4), (7, 3), (7, 2) and (8, 1)*

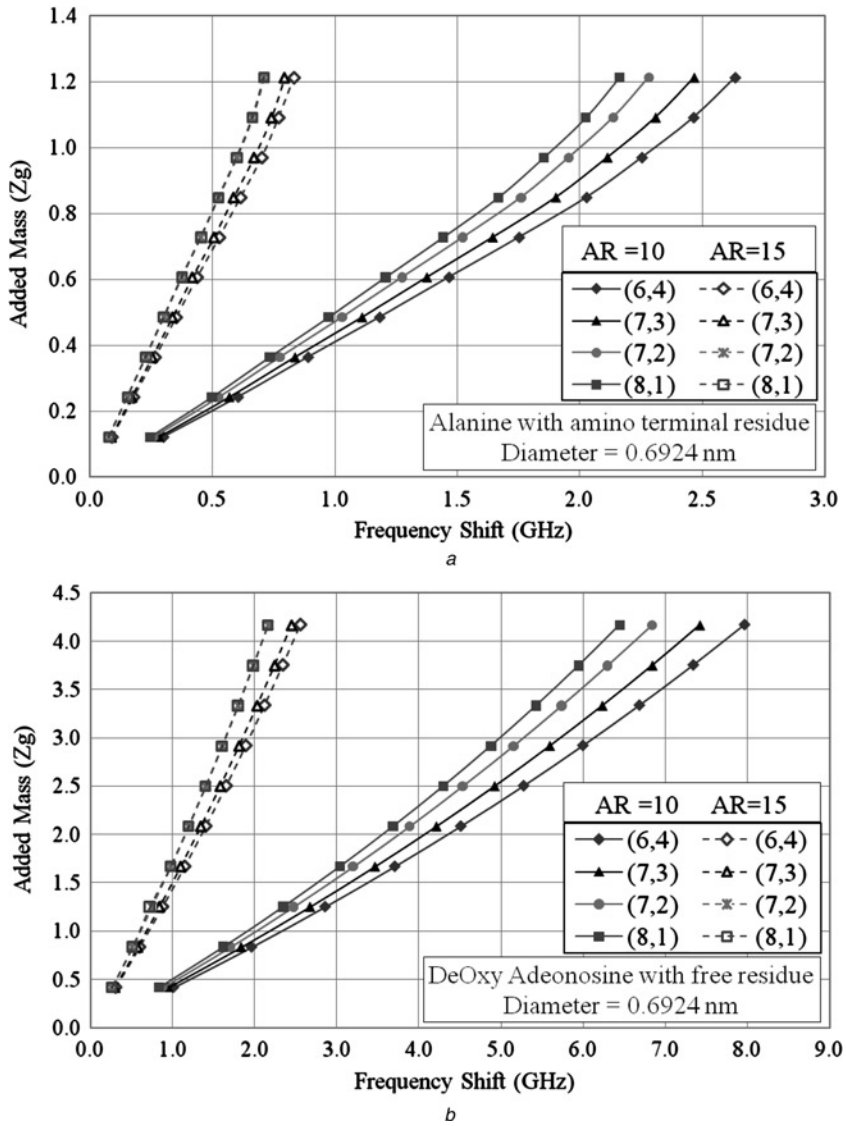

Fig. 7 *Resonant behaviour in terms of variation in frequency shift against added mass*

a Variation in frequency shift because of added molecules of alanine with amino terminal residue upto ten molecules
b Variation in frequency shift because of added molecules of deoxyadenosine with free residue upto ten molecules

higher structural mass for the nanotube of aspect ratio 15 compared with nanotube of aspect ratio 10. As the chirality of the nanotube in terms of chiral angle θ decreases the frequency shift decreases, for the particular magnitude of added mass at the free end of the nanotube and become more sensitive.

5.2.2 Effect of intermediate landing position of the considered biological objects: All the atoms of the nanotube vibrate at different amplitudes along the length of the nanotube. A mass that lands near the fast moving region has a much greater effect on resonant frequency and equivalent to a much greater mass arriving near the fixed end. Based on this conception, effect on resonant behaviour due to intermediate landing of the added mass along the length of nanotube needs to be explored for the resonant-based sensing applications. The higher-order vibrational modes need to be exploited because change in the resonant frequency also depends on how the nanotube moves at the landing point of mass [28]. The measurements made with higher-order modes could potentially take into account both the mass and landing position to be determined. Hence, detection and mensuration of the mass require investigation of the frequency shifts of the higher-order modes of vibration [22, 28]. Using the present FE model-based simulation approach, the deflection of all the atoms along the length of nanotube can be effectively analysed, by analysing the vibrational characteristics (frequencies and mode shapes) of higher-order modes of vibrations for cantilevered SWBNNT [29]. Considering this conception, cantilevered configuration of armchair form (4, 4) of SWBNNT of diameter 0.551 nm and length 9.99 nm is analysed for frequency shift of the fundamental modes of vibrations against different intermediate landing positions of the added mass. The frequency shift of different modes of vibrations; first bending, first twisting, first axial and first radial are considered to analyse different intermediate landing positions of the single molecule of alanine with amino terminal residue, having smaller mass compared with that of single molecule of deoxyadenosine with free residue, along the length of the nanotube.

Fig. 8*a* shows the deformation of nanotube for first fundamental mode of vibrations. The first bending mode has a half-sine shape as observed in a beam. The atoms in

doi: 10.1049/iet-nbt.2013.0012

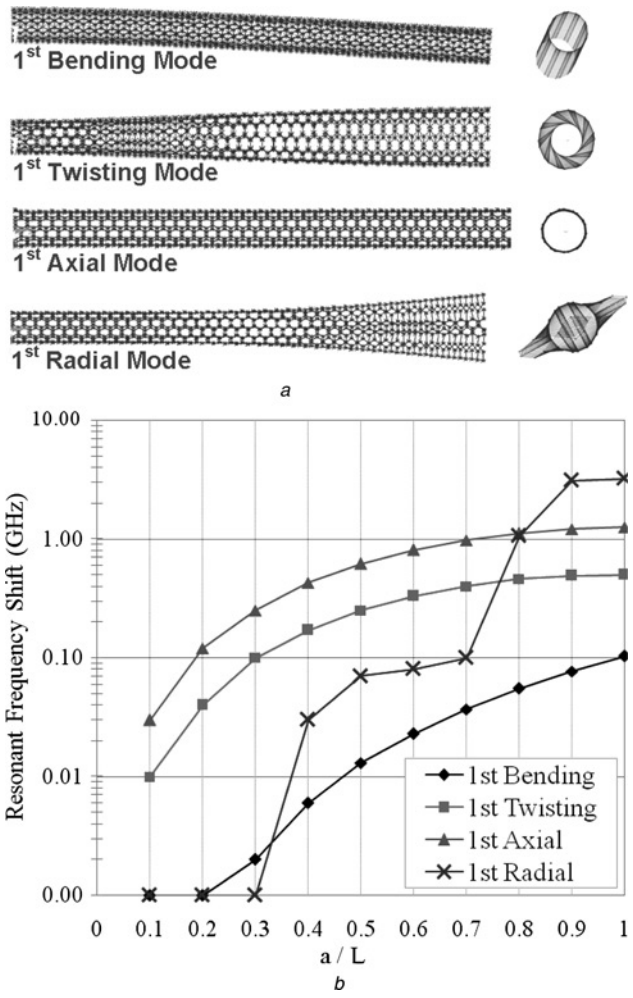

Fig. 8 *Fundamental modes of vibration and frequency shift against intermediate position of added mass along the length of SWBNNT of armchair form (4, 4), having diameter 0.551 nm and length of 9.99 nm*

a Different modes: first bending, first twisting, first axial and first radial [22]
b Frequency shift against intermediate landing position of attached mass along the length of cantilevered configuration of SWBNNT-based biosensor

twisting mode move in the circumferential direction with increase in radius of the SWBNNT along the length from the fixed end; all the atoms have the same circumferential movement and maximum increase in the radius is observed at the free end of the cantilevered configuration. The first axial mode is accompanied by simultaneous movement of all atoms along the longitudinal direction. In the first radial mode, the free end of the cantilevered configuration takes an elliptical shape. Fig. 8*b* shows the variation in frequency shift of considered basic modes of vibration against different intermediate positions of added mass along the length of the nanotube. The variation in frequency shift for the first twisting and first axial modes of vibration follow the same pattern of increase in frequency shift as added mass moves away from the fixed end with higher frequency shift for the first axial mode compared with that for the first twisting mode. At the position of the added mass nearer to the fixed end, upto 20% of the total length of nanotube the frequency shift for the first bending mode is zero and as the position of the added mass moves towards the free end the frequency shift for the first bending mode increases with the value less than that for the first twisting mode. The obtained results for variation in frequency shift for the first radial mode shows the jump like pattern with increase in frequency shift as added mass moves from the fixed end to the free end of the nanotube. For the position of the added mass nearer to the fixed end (upto 30% of the total length) the frequency shift for the first radial mode in zero, that is, there is no effect of added mass on the frequency of first radial mode of vibration, and for the position of the added mass between 40 and 70% of the total length from the fixed end of the nanotube, there is a jump in frequency shift and for the position of added mass nearer to the free end (greater than 70% of the length from fixed end), there is another jump in frequency shift for the first radial mode vibration. When the magnitude of attached mass changes, the frequency shift for the radial, axial and twisting modes will also follow the similar pattern of increase in frequency shift, when attached mass moves towards the free end of the nanotube, but with the different values of frequency shifts for particular landing positions of the attached mass. This effect on frequency shifts of higher-order modes of vibrations can be used to develop the algorithm for mass detection as well as identification of its landing position. Thus, the obtained results for frequency shift variation for higher-order modes of vibrations assist in detection and identification of the location of added biological objects along the length of SWBNNT based biosensors.

Using present atomistic FE-based modelling of SWBNNT dynamic analysis for the SWBNNT-based biosensor systems can be performed considering their resonant behaviour. However, BNNT have piezoelectric properties, and recently Zhang *et al.* [30] have analysed the effect of applied axial electric field on pre-buckling and buckling behaviours of BNNTs and nanosheets based on molecular mechanics approach. Zhang *et al.* [30] have reported that when the axial electric increases beyond a critical value (E_{cr}) an axial buckling occurs in zigzag nanotubes and a torsional buckling occurs in armchair nanotubes, and concluded that critical value of electric field (E_{cr}) decreases as the aspect ratio increases for both zigzag and armchair nanostructures. In future, using multiphysics approach, a more robust sensor systems using BNNTs can be proposed to incorporate piezoelectric properties along with their vibrational characteristics.

6 Conclusion

Using the present FE modelling-based simulation approach the feasibility of SWBNNT-based biosensor in terms of detection as well as identification of intermediate landing position of the biological object having mass of zeptogram-scale is exploded. Acceptable agreements between the obtained results using the present approach and the published computation results have been observed. The effect of chirality on the performance of SWBNNT-based biosensor suggests that the chirality in terms of chiral angle decreases the frequency shift decreases which means SWBNNT of having small value of chiral angle having higher sensitivity as compared with having higher value of chiral angle. The frequency shift analysis for higher-order modes of vibration can be used to develop an algorithm based on frequency shift to identify the intermediate landing position of the biological object along the length of nanotube. The obtained results may be useful to practically realise future SWBNNT-based biosensors.

7 References

1 Wong, S.S., Joselevich, E., Woolley, A.T., Cheung, C.L., Lieber, C.M.: 'Covalently functionalized nanotubes as nanometersized probes in chemistry and biology', *Nature*, 1998, **394**, p. 52

2 Cui, Y., Wei, Q.Q., Park, H.K., Lieber, C.M.: 'Nanowire nanosensors for highly sensitive and selective detection of biological and chemical species', *Science*, 2001, **293**, p 1289

3 Benyamini, H., Shulman-Peleg, A., Wolfson, H.J., Belgorodsky, B., Fadeev, L., Gozin, M.: 'Interaction of c(60) fullerene and carboxyfullerene with proteins: docking and binding site alignment', *Bioconjugate Chem.*, 2006, **17**, p. 378

4 Hong, R., Fischer, N.O., Verma, A., Goodman, C.M., Emrick, T., Rotello, V.M.: 'Control of protein structure and function through surface recognition by tailored nanoparticle scaffolds', *J. Am. Chem. Soc.*, 2004, **126**, p. 739

5 Mukhopadhyay, S., Scheicher, R.H., Pandey, R., Karna, S.P.: 'Sensitivity of boron nitride nanotubes toward biomolecules of different polarities', *J. Phy. Chem. Lett.*, 2011, **2**, pp. 2442–2447

6 Soto-Verdugo, V., Metiu, H., Gwinn, E.: 'The properties of small Ag clusters bound to DNA bases', *J. Chem. Phys.*, 2010, **132**, article id 195102

7 Shewale, V., Joshi, P., Mukhopadhyay, S., *et al.*: 'First-principles study of nanparticle-biomolecular interactions: anchoring of a (ZnO)12 cluster on nucleobases', *J. Phys. Chem. C*, 2011, **115**, p 10426

8 Hood, L., Heath, J.R., Phelps, M.E., Lin, B.: 'Systems biology and new technologies enable predictive and preventative medicine', *Science*, 2004, **306**, pp. 640–643

9 Chopra, N.G., Luyken, R.J., Cherrey, K., *et al.*: 'Boron-nitride nanotubes', *Science*, 1995, **269**, pp. 966–967

10 Zhi, C., Bando, Y., Tang, C., Golberg, D.: 'Immobilization of proteins on boron nitride nanotubes', *J. Am. Chem. Soc.*, 2005, **127**, (49), pp. 17 144–145

11 Ciofani, G., Raffa, V., Menciassi, A., Cuschieri, A.: 'Boron nitride nanotubes: an innovative tool for nanomedicine', *Nano Today*, 2009, **4**, (1), pp. 8–10

12 Adhikari, S., Chowdhury, R.: 'The calibration of carbon nanotube based bio-nano sensors', *J. Appl. Phys.*, 2010, **107**, (12), pp. 124 322 1–8

13 Panchal, M.B., Upadhyay, S.H., Harsha, S.P.: 'Mass detection using single walled boron nitride nanotube as a nanomechanical resonator', *NANO: Brief Rep. Rev.*, 2012, **7**, (4), pp. 1250029 1–11

14 Panchal, M.B., Upadhyay, S.H., Harsha, S.P.: 'Vibration analysis of single walled boron nitride nanotube based nanoresonators', *J. Nanotechnol. Eng. Med. Trans. SME*, 2013, **3**, (3), pp. 031004 1–5

15 Jiang, L.C., Zhang, W.D.: 'A highly sensitive nonenzymatic glucose sensor based on cuo nanoparticles-modified carbon nanotube electrode', *Biosens. Bioelectron.*, 2010, **25**, (6), pp. 1402–1407

16 Braun, T., Barwich, V., Ghatkesar, M.K., *et al.*: 'Micromechanical mass sensors for biomolecular detection in a physiological environment', *Phy. Rev. E*, 2005, **72**, article id 031907

17 Joshi, A.Y., Sharma, S.C., Harsha, S.P.: 'Zeptogram scale mass sensing using single walled carbon nanotube based biosensors', *Sens. Actuator A, Phys.*, 2011, **168**, pp. 275–280

18 Kuang, Z., Kim, S.N., Goodson, W.J.C., Farmer, B.L., Naik, R.R.: 'Biomimetic chemosensor: designing peptide recognition elements for surface functionalization of carbon nanotube field effect transistors', *ACS Nano*, 2010, **4**, (1), pp. 452–458

19 Farmanzadeh, D., Ghazanfary, S.: 'The effect of electric field on the interaction of glycine with (6, 0) single walled boron nitride nanotubes', *J. Serb. Chem. Soc.*, 2012, **77**, (0), pp. 1–14

20 Chowdhury, R., Adhikari, S.: 'Boron-nitride nanotubes as zeptogram-scale biosensors: theoretical Investigations', *IEEE Trans. Nanotechnol.*, 2011, **10**, (4), pp. 659–667

21 Dohn, S., Svendsen, W., Boisen, A.: 'Mass and position determination of attached particles on cantilevered based mass sensors', *Rev. Sci. Instrum.*, 2007, **78**, (10), article id 103303

22 Panchal, M.B., Upadhyay, S.H., Harsha, S.P.: 'An efficient finite element model for analysis of single walled boron nitride nanotube-based resonant nanomechanical sensors', *NANO: Brief Rep. Rev.*, 2013, **8**, (1), pp. 1350011 1–16

23 Boldrin, L., Scarpa, F., Chowdhury, R., Adhikari, S.: 'Effective mechanical properties of hexagonal boron nitride nanosheets', *Nanotechnology*, 2011, **22**, article id 505702

24 Moon, W.H., Hwang, H.J.: 'Molecular mechanics of structural properties of boron nitride nanotubes', *Phys. E*, 2004, **23**, pp. 26–30

25 Chopra, N.G., Zettl, A.: 'Measurement of the elastic modulus of a multi walled boron nitride nanotube', *Solid State Commun.*, 1998, **105**, (5), pp. 297–300

26 Suryavanshi, A.P., Yu, M.F., Wen, J., Tang, C., Bando, Y.: 'Elastic modulus and resonance behavior of boron nitride nanotubes', *Appl. Phys. Lett.*, 2004, **84**, (14), pp. 2527–2529

27 Timoshenko, S.P., Gere, J.M.: 'Theory of elastic stability' (McGraw-Hill, 1961)

28 Knobel, R.G.: 'Mass sensors: weighing single atoms with a nanotube', *Nature Nanotechnol.*, 2008, **3**, pp. 525–526

29 Panchal, M.B., Upadhyay, S.H.: 'Vibrational analysis of zigzag and armchair fixed-free single walled boron nitride nanotubes: atomistic modeling approach', *Curr. Nanosci.*, 2013, **9**, (2), pp. 254–261

30 Zhang, J., Wang, C.W., Adhikari, S.: 'Molecular structure-dependent deformations in boron nitride nanostructures subjected to an electric field', *J. Phys. D, Appl. Phys.*, 2013, **46**, (23), pp. 235303 1–6

doi: 10.1049/iet-nbt.2013.0012